

Exploring the Potential of Plumbagin as an Activator of Caspase 3 for Non-small Cell Lung Carcinoma: A Comprehensive *in silico* Study

Mohd Saeed^{1,*}, Munazzah Tasleem², Samra Siddiqui³, Tarun Kumar Upadhyay^{4,*}, Tulika Bhardwaj⁵, Md Jahoor Alam¹, Saad Saeed Alqathani⁶, Fevzi Bardakci¹, Nujud Almuzaini¹, Rania Abdeen Hussain Abdalla⁷, Ambreen Shoab⁸

¹Department of Biology, College of Sciences, University of Hail, Hail, SAUDI ARABIA.

²Department of Biomedical Imaging and Electrophysiology, School of Electronic Science and Engineering, University of Electronic Science and Technology of China, Chengdu, Sichuan, CHINA.

³Department Health Services Management, College of Public Health and Health Informatics, University of Hail, Hail, SAUDI ARABIA.

⁴Department of Biotechnology, Parul Institute of Applied Sciences and Research and Development Cell, Parul University, Vadodara, Gujarat, INDIA.

⁵Department of Agricultural, Food and Nutritional Sciences, University of Alberta, Edmonton, AB T6G 2P5, CANADA.

⁶Department of Clinical Pharmacy, College of Pharmacy, King Khalid University, Abha, SAUDI ARABIA.

⁷Department of Obstetrics and Gynecology, College of Medicine, University of Hail, Hail, SAUDI ARABIA.

⁸Department of Clinical Pharmacy, College of Pharmacy, Jazan University, Jazan, SAUDI ARABIA.

ABSTRACT

Caspase-3 regulates apoptosis, and its deregulation in Non-Small Cell-Lung Carcinoma (NSCLC), and contributes to tumour growth and therapeutic resistance. Significant resistance to chemotherapy and radiation therapy, which are two frequently used treatment modalities for lung cancer, is linked to the decreased activity of caspase-3 in NSCLC. Preclinical and early clinical investigations, for example, have shown potential for targeting specific biochemical pathways involved in caspase-3 regulation, such as the Bcl-2 family of proteins or the Inhibitor of Apoptosis Proteins (IAPs). However, this study investigates the activation potential of plumbagin, a potential naphthoquinone, towards Caspase-3, which in turn targets the progression of NSCLC. The potential of naphthoquinones has already been explored and experimentally validated by several researchers in cancer-targeted drug discovery-based studies. This study focuses on exploring the physicochemical and ADMET properties of plumbagin prior to molecular docking. This renders the binding energy of the plumbagin-caspase-3 docked complex at -10.13 kcal/mol. Further, MD simulations validated the potential of Plumbagin to serve as a promising target for drug discovery against caspase-3 by analysing the computed trajectories. Given that naphthoquinones are preferred drug candidates, discovering natural chemicals that act as caspase-3 activator is a key step towards developing viable drugs for NSCLC.

Keywords: Non-Small Cell-Lung Cancer (NSCLC), Caspase-3, Plumbagin, BOILED EGG Plot analysis, ADMET/Tox, Molecular docking, MD simulation.

Correspondence:

Dr. Mohd Saeed

Department of Biology, College of Sciences, University of Hail, Hail-2240, SAUDI ARABIA.

Email: mo.saeed@uoh.edu.sa

Dr. Tarun Kumar Upadhyay

Department of Biotechnology, Parul Institute of Applied Sciences and Research and Development Cell, Parul University, Vadodara-391760, Gujarat, INDIA.

Email: tarun_bioinfo@yahoo.co.in

Received: 20-10-2023;

Revised: 19-12-2023;

Accepted: 22-01-2024.

INTRODUCTION

Cancer is a prominent contributor to global mortality rates. In the year 2020, the United States witnessed the identification of approximately 1.8 million novel instances of cancer, with a corresponding mortality rate of 606,520 individuals succumbing to this disease.¹ It is projected that the number of fatalities in the United States due to lung cancer in 2021 will surpass the

combined mortality resulting from prostate, breast, and colon cancers. The estimated figure stands at 135,760 deaths.^{2,3} In the year 2020, Saudi Arabia recorded a total of 27,885 newly diagnosed cases of cancer, along with 13,069 reported deaths attributed to this disease. Out of the total population, a total of 1157 individuals were diagnosed with lung cancer, while 1001 deaths were reported. Lung cancer has been identified as the predominant form of cancer among males in Saudi Arabia.⁴ Lung cancer continues to be the biggest cause of fatalities from cancer in the United States and worldwide. Non-Small Cell-Lung Cancer (NSCLC) is relatively insensitive to chemotherapy and accounts for about 85% of all lung cancer cases reported. Regrettably, over 80% of all patients diagnosed with NSCLC die eventually due to



DOI: 10.5530/ijper.58.2.59

Copyright Information :

Copyright Author (s) 2024 Distributed under Creative Commons CC-BY 4.0

Publishing Partner : EManuscript Tech. [www.emanuscript.in]

the disease within 5 years.^{5,6} Despite significant advancements in platinum-based chemotherapy, the emergence of novel molecularly targeted therapies, and the promising potential of immunotherapies, the overall survival advantage for lung cancer patients still remains a challenge. Poor outcomes and relapses following NSCLC diagnosis in conjunction with adverse effects of treatments for months to years following chemo-/radiotherapy indicate the need for new treatment options for this often-fatal disease. Despite 2 decades of chemotherapy for advanced NSCLC, the survival benefit remains modest.⁷ It is a high time that new strategies be developed for more effective lung cancer treatment using simple and effective interventions.

The protease enzyme family known as caspases regulates apoptosis and is used for many purposes besides just cell death. To comprehend the functions of caspases in health and disease, as well as to find innovative therapeutic approaches that target these enzymes, it is essential to comprehend the processes of caspase activation and control.⁸ Cells commonly contain inactive caspases, which can undergo activation through a sequence of proteolytic cleavage processes triggered by various signals such as DNA damage, the absence of growth factors, or immunological signaling.⁹ Once activated, caspases cleave and activate downstream substrates, causing cellular changes associated with apoptosis such as DNA damage, nuclear condensation, and cell shrinkage. Among all types of caspase proteins, Caspase-3 is of utmost importance due to its active involvement in NSCLC.¹⁰ Cleavage occurs on the carboxy side of the second aspartic acid residue (between D and G) in the peptide DEVDG (Asp-Glu-Val-Asp-Gly), which has been found to be the preferred substrate for caspase-3.¹¹ Gly238 and Cys285's amides polarize the scissile bond carbonyl group by donating H bonds to the carbonyl oxygen.¹²

Roots of the plant *Plumbago zeylanica* L. yield the naphthoquinone plumbagin (5-hydroxy-2-methyl-1,4-naphthoquinone).^{13,14} Its various pharmacological activities have been reported which include anti-inflammatory activities, anti-cancer,¹⁵ antidiabetic activities, antioxidant, and antibacterial activities, antifungal, anti-atherosis, and analgesic activities.^{16,17} Lately, much attention has been paid to revealing its potential as antimicrobial and anticancer.¹⁸ However, studies of the mechanism of action in the suppression of tumour growth are scanty. There are only a few studies currently available on its mechanism; therefore, this study is planned to demonstrate its full potential as a potent anticancer compound and reveal its mechanism in inhibiting the growth of cancer cells. In this study, the binding mode of plumbagin with caspase-3 was elucidated utilizing several biophysical and computational methodologies viz. molecular docking. Finally, MD simulation studies substantiate the docking-based findings and provide detailed information regarding the interacting amino acid residues.

MATERIALS AND METHODS

Selection of target protein structure

The three-dimensional structure of the target protein is obtained from the UniProt database, accessible at <https://www.uniprot.org/>. The AlphaFold protein structure database has been utilized to generate protein structures that are both highly accurate and validated¹⁹ within UniProt is mined with respective ID (AF-P42574-F1) for the Caspase-3 (*Homo sapiens*).

Ligand selection and ADMET analysis

The 3D structure of the plumbagin²⁰ compound was retrieved from PubChem²¹ and evaluated for drug-likeness using Discovery Studio [Dassault Systems, BIOVIA Corp., San Diego, CA, USA, v 21.1]. The compound was assessed for Lipinski rule of 5, and ADMET properties) using ADME and TOPKAT modules from Discovery Studio. The ADMET and TOPKAT modules within the DS software are employed for the evaluation of ADMET properties in compounds. These properties encompass various aspects including water solubility, blood-brain barrier (BBB) permeability, hepatotoxicity, human intestinal absorption, plasma protein binding (PPB) levels, rodent carcinogenicity, AMES mutagenicity, and developmental toxicity potential.^{22,18}

Analysis of the BOILED EGG plot

The utilization of the Estimate D permeation method, also known as BOILED-Egg, within the brain or intestinal tract, represents a valid predictive model for evaluating the lipophilicity and polarity of ligands. This method offers a precise statistical framework for examining the characteristics associated with the bioavailability of ligand molecules. The prediction of physical and chemical properties, such as the permeability of the blood-brain barrier and gastrointestinal absorption, can be inferred using fried eggs as a model. The utilization of the Swiss ADME online service is prevalent in the generation of BOILED plots, a necessary component in the realm of drug research and discovery.²³

Molecular docking studies of Plumbagin-Caspase 3

The structural docking of the energy-minimized 3D ligand and target protein was performed using AutoDock version 4.2. The 3D structures of the ligands and protein were converted from .pdb format to .pdbqt format using the appropriate Python script developed for this purpose in AutoDock Tools.²⁴ The appropriate grid box for the target protein at the individual level was determined manually by assessing the critical residues within the target protein. These critical residues include the catalytic residues and substrate binding residues, which play a vital role in the function and specificity of the protein under consideration. The docking simulations were conducted utilizing the Lamarckian Genetic algorithm (LGA), with the active site positioned at the center of the grid box. The binding energy conformation of the ligand was determined using default parameters, which included

2,500,000 energy assessments, 27,000 generations, a population size of 150, a gene mutation rate of 0.02, and a crossover rate of 0.8. These parameters were applied in 10 separate runs. The software PyMOL was employed to visualize the data.²⁵

MD simulation Studies

A Molecular Dynamics (MD) simulation was conducted using GROMACS 5.1.5 software and the GROMOS96 54a7 force field to evaluate the stability of the protein-ligand complexes in the docked complex.²⁶ The topology for Plumbagin was generated using version 3.0 of the Automated Topology Builder (ATB) accessed through the website atb.uq.edu.au. The protein-ligand mixture was introduced into the central region of a cubic periodic box, followed by the addition of Simple Point Charge (SPC) fluids to solvate the system. Subsequently, the system's net charge was equilibrated through the introduction of Na⁺ and Cl⁻ ions. The preservation of energy was achieved through the utilization of the steepest descent algorithm. Subsequently, the system underwent an NVT simulation, wherein an infinite number of particles, volume, and temperature were maintained. The simulation involved heating the system to a temperature of 310 K over duration of 500 picoseconds, with each time step being 2 femtoseconds. In the NPT simulation lasting 500 picoseconds with a time step of 2 femtoseconds, the pressure was systematically raised to 1 bar while maintaining a constant number of particles and temperature. The temperature of the v-rescale method was maintained at a constant value of 310 K. The pressure was controlled at a constant value of 1 bar through the utilization of the Parrinello-Rahman pressure coupling technique.²⁷ The time constants for coupling temperature and pressure were maintained at a constant value of 0.1 ps and 2 ps, respectively. The long-range electrostatic interactions were calculated using the Particle Mesh Ewald (PME) method with a grid spacing of 0.16 nm and employing fourth-order cubic interpolation.

The calculation employed in this study is the Molecular Mechanics Generalized Born and Surface Area (MM-GBSA) method

The binding free energy (ΔG_{bind}) of docked complexes was determined through Molecular Dynamics (MD) simulations, employing the Molecular Mechanics Generalized Born Surface Area (MM-GBSA) module. The determination of the binding free energy was conducted utilizing the OPLS-AA/L force field, the VSGB solvent model, and rotamer search techniques. The MD trajectories were sampled at regular intervals of 10 nanoseconds following the completion of the molecular dynamic's simulation.

RESULTS

ADMET analysis of plumbagin for drug-like characteristics

The drug-like characteristics of plumbagin were evaluated using the Lipinski and Veber rule. The ADMET properties of a molecule are of considerable importance in the field of drug discovery, as they are primarily accountable for the failure of medicines in approximately 60 percent of clinical trial instances.²⁸ A molecule exhibiting a favorable Absorption, Distribution, Metabolism, and Excretion (ADME) profile is capable of being absorbed through the gastrointestinal system and subsequently entering circulation. It undergoes processing by metabolic enzymes and is ultimately eliminated from the body. Importantly, this molecule does not disrupt or impede normal biological processes.²⁹ The ADMET descriptors module within the DS software assesses several key properties of a drug-like molecule, including AlogP98, PSA (polar surface area), Plasma Protein Binding (PPB), hepatotoxicity, CYP2D6 enzyme inhibition, aqueous solubility, Blood-Brain Barrier (BBB) permeability, and intestinal absorption.³⁰ A linear regression model was employed to estimate the aqueous solubility in water at a temperature of 25°C. Following oral administration, the absorption and solubility levels of the compounds are indicative of their potential for absorption in the human intestine and their likelihood of being effective as drugs. In the context of intestinal absorption, it is desirable for the values to be equal to or greater than zero, indicating good absorption⁵ or moderate absorption.³¹ Similarly, for aqueous solubility, the optimal values are 3 and 4.^{32,33} The compound's hydrophilicity is assessed based on its AlogP98 value, whereby a value greater than 5 indicates a high level of absorption or permeability. Pharmacokinetic factors, such as the presence of P-glycoprotein efflux transporters, can significantly impact drug bioavailability. Compounds with a prostate-specific antigen³⁴ value of 140 Å or less exhibit the capability of passive absorption, leading to a significant increase in their oral bioavailability. Plumbagin exhibited a notable degree of absorption and demonstrated favorable solubility in aqueous environments. The BBB level is a metric used to assess the extent of drug permeation into the Central Nervous System (CNS) following oral administration. The avoidance of Blood-Brain Barrier (BBB) penetration is a desirable characteristic for a drug, as crossing the BBB can have detrimental effects on the Central Nervous System (CNS). Consequently, therapeutic molecules possessing Blood-Brain Barrier (BBB) values of 3 or 2 (indicating low or medium permeability) are commonly considered optimal for administration.²⁸

The assessment of a drug compound's hepatotoxicity level involves evaluating its capacity to induce liver damage in a dose-dependent manner. This information is commonly employed to predict drug toxicity. The metabolism of drugs is regulated by CYP450 enzymes and their corresponding isoforms. The inhibition of these detoxifying enzymes can lead to the manifestation of toxic

effects.³⁵ The CYP2D6 enzyme constitutes a mere 2% of the total Cytochrome P450 (CYP) content. However, it is responsible for the biotransformation of approximately 20% of pharmaceuticals that undergo hepatic metabolism. A significant proportion exceeding 80% of pharmaceutical compounds utilized in clinical trials undergo metabolic processes primarily mediated by five distinct Cytochrome P450 (CYP) isoforms, namely 3A4, 2D6, 2C19, 2C9, and 1A2. The investigation did not find any evidence of Plumbagin inhibiting the CYP2D6 enzyme, and no significant hepatotoxicity resulting from drug interactions was observed in the liver. The Plasma Protein Binding (PPB) assay quantifies the affinity of a pharmaceutical compound to bind with proteins present in the bloodstream. The effectiveness of the drug may be influenced by the extent of its binding. The obtained PPB values were classified as "false" and "true" for drug molecules that are "poorly" and "highly bounded," respectively, as presented in Table 1.

The findings from the TOPKAT and ADMET analyses indicate that the projected carcinogenicity values of the plumbaginis fall within the anticipated range. However, it is important to note that there is a potential risk of mutagenicity associated with these compounds. The study demonstrated the ability to elicit both mild and strong skin irritation. Table 2 presents a summary of additional toxicity screening attributes, including the Rat inhalation LC₅₀, Rat of Oral LD₅₀, Fathead minnow LC₅₀, and Daphnia EC₅₀.

BOLIED EGG plot analysis

Besides the prediction of ADME (Absorption, Distribution, Metabolism, and Excretion), the presence of adverse pharmacokinetic properties plays a role in the toxicity and efficacy concerns of small molecules. This method, which is based on two physicochemical descriptors, specifically WLOGP and TPSA, is characterized by its intuitive nature. Figure 1 illustrates the pharmacokinetic properties of the Plumbagin BOILED EGG plot, which exhibits two favorable characteristics: passive gastrointestinal absorption and penetration of the Blood Brain Barrier. Plumbagin is anticipated to possess the ability to penetrate the blood-brain barrier and is not susceptible to active efflux mechanisms. The presence of a red dot signifies that the molecule is subject to extrusion from the central nervous system through the action of Glycoprotein. In the conducted study, it was determined that plumbagin exhibited the highest efficacy as an anti-cancer medication. Additionally, it is necessary to conduct *in vitro* and *in vivo* research studies on the natural ligand in order to validate the findings of this study.

Molecular Docking and Interaction Studies

The utilization of molecular docking has become increasingly significant as a computational technique for the virtual screening of potential drug candidates. The utilization of high-throughput screening techniques facilitates expedited drug development

processes through the assessment of numerous compounds' activity against specific proteins. This approach expedites the identification of candidate ligand-protein interactions within a significantly shorter timeframe, thereby resulting in reduced expenses associated with laboratory-based screening procedures.³⁶ The objective of this study was to assess the binding affinities and intra-molecular interactions between the target proteins and plumbagin, with the aim of eliminating any erroneous positive results.³⁷ Molecular docking studies serve to determine the anticipated binding modes of the ligand within the active site of the protein. Consequently, the computed value for the binding energy was -10.13 kcal/mol. The computed energies corresponding to each association are presented in Table 3 and visually represented in Figure 2.

MD Simulation Studies

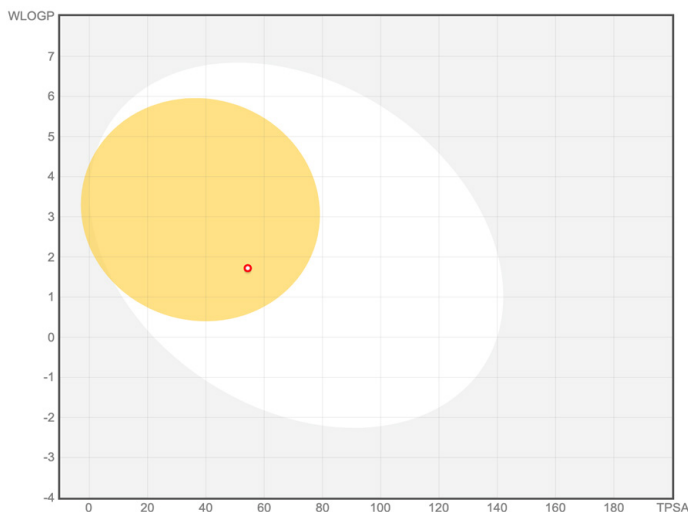
In order to assess the stability of the protein-ligand complexes, Molecular Dynamics (MD) simulations were conducted for a duration of 200 nanoseconds. The docked complex, specifically the Caspase 3-Plumbagin complex, was analyzed using various parameters including the Radius of gyration (Rg), Root Mean Square Deviation (RMSD), and Root Mean Square Fluctuations (RMSF) of the Cα atoms.³⁸ During the course of the Molecular Dynamics (MD) simulation, the Radius of gyration (Rg) of the protein-ligand docked complexes exhibits minimal fluctuations, as depicted in Figure 3b. The mean Rg value of the docked complex is 2.313±0.043 nm. Additionally, it can be observed that the Root Mean Square Deviation (RMSD) value of the Cα atoms in the docked complexes reaches a stable state after

Table 1: ADME properties of Plumbagin.

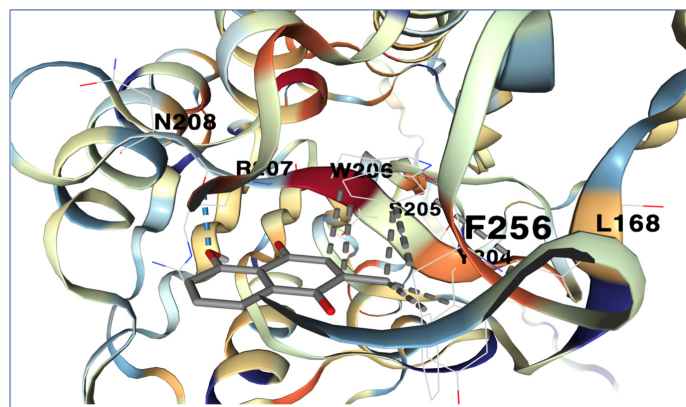
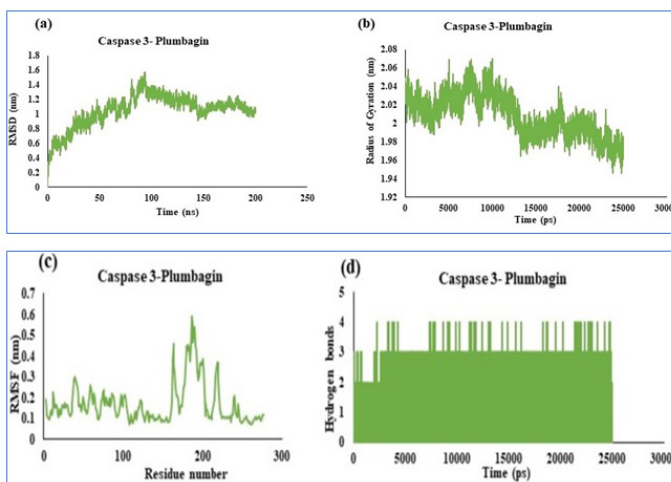
Properties	Parameters
Molecular_Weight	188.179
ALogP	1.962
Num_RotatableBonds	0
Molecular Polar Surface Area	54.37
Num_H_Acceptors	3
Num_H_Donors	1
Num_Rings	2
Num_Aromatic Rings	1
ADMET Solubility_Level	3
ADMET_Unknown_AlogP98	0
ADMET BBB_Level	2
ADMET_EXT_CYP2D6	FALSE
ADMET_EXT_Hepatotoxic	FALSE
ADMET_Absorption_Level	0
ADMET_EXT_PPB	FALSE
ADMET_AlogP98	1.962
ADMET_PSA_2D	55.417

Table 2: Plumbagin Toxicity prediction.

Properties	Parameters
TOPKAT_Mouse_Female_NTP_Prediction	Non-Carcinogen
TOPKAT_Mouse_Male_NTP_Prediction	Carcinogen
TOPKAT_Rat_Female_NTP_Prediction	Carcinogen
TOPKAT_Rat_Male_NTP_Prediction	Carcinogen
TOPKAT_Mouse_Female_FDA	Non-Carcinogen
TOPKAT_Mouse_Male_FDA	Non-Carcinogen
TOPKAT_Rat_Female_FDA	Non-Carcinogen
TOPKAT_Rat_Male_FDA	Single-Carcinogen
TOPKAT_WOE_Prediction	Non-Carcinogen
TOPKAT_Ames_Prediction	Mutagen
TOPKAT_DTP_Prediction	Toxic
TOPKAT_Rat_Oral_LD ₅₀	0.76507 g/kg_body_weight
TOPKAT_Rat_Inhalational_LC ₅₀	4953.96 mg/m ³ /hr
TOPKAT_Skin_Irritancy	None
TOPKAT_Skin_Sensitization	Strong
TOPKAT_Ocular_Irritancy	Mild
TOPKAT_Aerobic_Biodegradability	Degradable

**Figure 1:** Decoding Plumbagin's Passage: Analyzing Passive Gastrointestinal Absorption and Brain Penetration using WLOGP (Atomic LogP) and TPSA with the BOILED-Egg Method.

20 nanoseconds (Figure 3a), exhibiting minimal fluctuations throughout the duration of the simulation. The average Root Mean Square Deviation (RMSD) value of Caspase 3-Plumbagin is 0.618 ± 0.018 nm within the time interval of 80 ns to 150 ns, and it attains stability at 200 ns. Figure 3c illustrates the RMSF (Root Mean Square Fluctuation) value per residue in the docked complex. The residues 163, 219, and those within the range of

**Figure 2:** Visualization of interacting residues of docked complex Caspase-3 and Plumbagin using PyMOL.**Figure 3:** (a) RMSD, (b) Radius of gyration, (c) RMSF and (d) Hydrogen bond analysis of Caspase 3-Plumbagin complex.

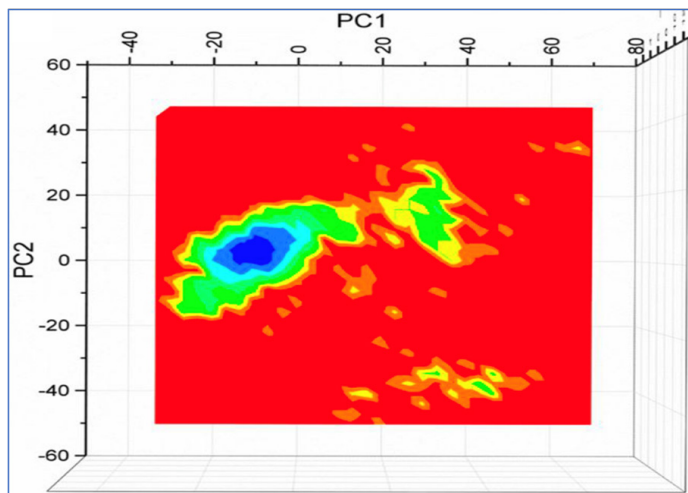
183-199 exhibit significant fluctuations in their trajectory. The docking outcome indicated the formation of multiple bonds, including hydrogen bonds and hydrophobic bonds, with the receptor. Subsequently, the stability of these bonds was further examined through analysis of the dynamic simulation trajectory. The results obtained from the dynamic simulation trajectory indicate that plumbagin maintains hydrogen bonds with Glu124, Lys137, Thr140, Arg164, Ile187, Pro188, Glu190, Tyr195, and Tyr197 (Figure 3d).

Molecular Mechanics Generalized Born and Surface Area (MMGBSA) calculation

It enables the estimation of Caspase-3-Plumbagin's binding free energy and additional non-bonded interaction energies would function. The docked complex has combined energy of -23.7763 kcal/mol. The non-bonded interactions such as G_{bind} Coulomb (-11.2265), G_{bind} Covalent (-0.11765), G_{bind} H bond (-0.81427), G_{bind} Lipo (-7.26116), G_{bind} SolvGB (2.66123), and G_{bind} vdW (-12.44232) have an impact on G_{bind} . The energies of the G_{bind} vdW, G_{bind} Lipo, and G_{bind} Coulomb interactions had the most impact on the average binding energy of all interactions. Covalent

Table 3: Computed binding energies of the docked complexes Caspase 3-Plumbagin.

Complex	Binding energy (kcal mol ⁻¹)	Docked energy (kcal mol ⁻¹)	Inter molecular energy (kcal mol ⁻¹)	Torsional energy (kcal mol ⁻¹)	Internal energy (kcal mol ⁻¹)	RMSD (Å)	Interacting residues
Caspase 3-Plumbagin	-10.13	-4.10	-3.09	0.77	-0.1	70.263	W206, R207, Y204, F256, L168, N208, S205

**Figure 4:** Free Energy Landscape of Caspase-3 and Plumbagin docked complex.

bonds demonstrated unfavourable energy contributions in each of the complexes, which prevented binding. The acquisition of the binding pocket is improved through conformational changes occurring at short time intervals, which are facilitated by interactions with residues that promote higher stability and enhanced binding energy.

The collective movement of the plumbagin complexed with caspase-3 is illustrated by PCA analysis. Protein flexibility and rigidity influences protein functionality, and the collective motion of the docked complex throughout the simulation time is computed and related free energy landscape is depicted in Figure 4. This plot infers the most possible conformations of the Caspase-3-Plumbagin complex in its lowest state.

DISCUSSION

Lung cancer ranks as the third most commonly occurring form of cancer globally, primarily originating in the cellular linings of the respiratory passages. The incidence rate of lung cancer exhibits geographical variations, as well as disparities in accordance with the World Health Organization (WHO). Populations characterized by high rates of smoking or exposure to environmental toxins tend to exhibit higher rates of lung cancer.³⁹ Symptoms associated with lung cancer encompass a persistent cough, chest discomfort, dyspnea, unintended weight loss, fatigue,

and recurrent respiratory ailments.⁴⁰ There are two primary types of lung cancer, namely Small Cell Lung Cancer (SCLC) and Non-Small Cell Lung Cancer (NSCLC). NSCLC is responsible for approximately 85% of all reported cases.⁴¹ In addition to lifestyle choices, occupational smoking, exposure to carcinogens, and genetic predisposition are the primary etiological factors contributing to the development of Non-Small Cell Lung Cancer (NSCLC).⁴² In light of the distinct attributes of the malignancy and the patient's clinical state, individualized therapeutic interventions are anticipated to yield favorable outcomes, in conjunction with surgical intervention and radiation therapy. The findings from the ADMET (Absorption, Distribution, Metabolism, and Excretion) analysis conducted on plumbagin offer significant insights into its pharmacological and toxicological characteristics, thereby illuminating its potential as a viable candidate for drug development. Plumbagin exhibits potential as a viable pharmaceutical candidate due to its compliance with the Lipinski and Veber criteria. The molecular weight, lipophilicity (AlogP), and polar surface area³⁴ of the compound all adhere to acceptable parameters. The drug-like properties exhibited by plumbagin indicate its potential for oral bioavailability, a crucial requirement in the development of pharmaceuticals. Plumbagin exhibits a notable capacity for absorption, as evidenced by its absorption level of 0, which suggests a high degree of intestinal absorption. Additionally, the drug's aqueous solubility level of 3 contributes to its potential as a pharmaceutical agent. The aforementioned characteristics are crucial for achieving proficient verbal communication, thereby establishing plumbagin as a promising contender for pharmaceutical advancement. The lack of substantial hepatotoxicity and inhibition of the CYP2D6 enzyme observed with plumbagin provides a sense of reassurance. The issue of hepatotoxicity holds significant importance in the field of drug development, while the inhibition of CYP2D6 can result in potential drug interactions.⁴³ The obtained results mitigate concerns pertaining to hepatotoxicity and the possibility of drug-drug interactions, thereby enhancing the compound's safety profile. The low Plasma Protein Binding (PPB) of plumbagin suggests that it exhibits restricted affinity for binding with plasma proteins. This attribute is beneficial as it diminishes the probability of interactions that may impact the efficacy of drugs. The favorable pharmacokinetic properties of plumbagin may be attributed to its low Plasma Protein Binding (PPB) capacity.⁴⁴ The toxicity assessment indicates that

plumbagin carries a potential risk of mutagenicity and mild skin irritation. Moreover, the evaluation of the LC_{50} for rat inhalation, LD_{50} for rat oral administration, LC_{50} for fathead minnows, and EC_{50} for *Daphnia* offers significant data that can be utilized in safety assessments during subsequent preclinical and clinical investigations.⁴⁵ In conclusion, the assessment of the Absorption, Distribution, Metabolism, Excretion, and Toxicity (ADMET) properties of plumbagin indicates a favorable perspective regarding its suitability as a pharmaceutical candidate. The compound's advantageous drug-like properties, such as efficient absorption, favorable solubility, and moderate blood-brain barrier permeability, make it a promising candidate for the development of orally administered drugs. In addition, the lack of notable hepatotoxicity and inhibition of CYP2D6 contributes to the improved safety profile of the substance. Nevertheless, it is imperative to recognize the potential hazards of mutagenicity and skin irritation that are linked to the use of plumbagin. The aforementioned findings underscore the necessity of conducting thorough toxicity assessments and additional preclinical investigations in order to ascertain the complete safety and efficacy of the compound.

The application of natural compounds for cancer treatment has gained attention over commercial treatment due to reduced side effects, anti-oxidative and immune-boosting properties, and availability and affordability.¹ Their innate ability to reduce related symptoms, which in turn provides respite and encourages well-being, complements, and enhances the effects of traditional cancer treatments.^{46,47} Therefore, this study investigates the activation potential of plumbagin, a potential naphthoquinone towards NSCLC-related potential drug target. Naphthoquinones are a topic of interest to scientists since they exhibit an array of anti-inflammatory and anti-cancer characteristics. As evidence, studies and reports on the inhibition potential of naphthoquinones in the treatment of several infectious diseases, neurological disorders, and cardiovascular diseases have already been conducted.⁴⁸

Plumbagin, a naturally derived naphthoquinone compound, exhibits promising anti-cancer properties through its ability to induce programmed cell death (apoptosis), hinder cell proliferation, and regulate various signaling pathways. The substance demonstrates anti-inflammatory characteristics, potentially aiding in the activation of inflammation-related mechanisms associated with the development and spread of tumors.⁴⁹ Seshadri *et al.* reported the potential of plumbagin in inducing caspase-3-dependent apoptosis involving the mitochondria through ROS generation in human peripheral blood lymphocytes.⁵⁰ Plumbagin targets mitochondrial-mediated ROS production and activates caspase-9 to cause apoptosis in lung cancer cells.¹⁶ Plumbagin has been observed to effectively activate signaling molecules that are consistently activated in various types of human cancers. Consequently, it has been extensively utilized

as a therapeutic target for cancer treatment, specifically targeting phosphatidylinositol-4,5-bisphosphate 3-kinase (PI3K),⁵¹ AKT,⁵² anti-apoptotic protein B cell lymphoma-2 (Bcl-2),⁵³ NF- κ B,⁵⁴ and Stat3.⁵⁵ A systematic pharmacological study for colorectal cancer treatment by application of plumbagin includes computationally intensive workflows and docking based platforms.⁵⁶ Computational analysis infers the ADMET prediction and BBB penetration capability of Plumbagin. Blood brain barrier plays a crucial role in cancer treatment when subjected to therapeutic delivery of drugs to brain⁵⁷ and central nervous system.⁵⁸ Efficacy of systematic chemotherapeutic agents is limited by low penetration in central nervous system⁵⁹ and active efflux from the same.⁶⁰ However, plumbagin shows the capability to pass BBB localised to tumour lesions in case of NSCLC treatment. Further molecular docking revealed that Plumbagin-Caspase-3 docked complex exhibits a binding energy of -10.13 kcal/mol. W206 and R207 interact with methylene substituent at position C7. L168 form hydrogen bonds with C3 and C5 position. Y204, F256 forms interaction with naphthalene ring at C4 position. The benzene ring at the C-5 position of the hydroxyl group forms the primary hydrogen bonding interaction, which can associate with the key chain consisting of oxygen atoms in N208 and S205. The analysis reveals that a significant proportion of active sites are located within the substrate pocket, indicating its potential as a viable therapeutic target.⁶¹

The stability of protein-ligand interactions was further investigated through the utilization of molecular dynamics simulations. The protein target's backbone structural framework was used to generate Root Mean Square Deviation (RMSD) graphs for time points at 200 nanoseconds. A mean Root Mean Square Deviation (RMSD) value of 0.637 ± 0.81 nm was calculated. The Root Mean Square Deviation (RMSD) values were observed to increase until the 3-nanosecond mark, after which they reached a state of stability with minimal fluctuations persisting throughout the remaining duration. Based on the findings reported in the Dictionary of Secondary Structure of Proteins (DSSP), it is widely believed that a majority of binding sites exhibit an alpha-helix conformation, whereas active sites are typically located within the substrate pocket. The flexibility of each residue in a protein-ligand docked complex was investigated by employing residue-based Root Mean Square Fluctuations (RMSF). Due to the absence of structural data pertaining to the target protein, there is considerable variation in the Root Mean Square Fluctuation (RMSF) values observed for the initial 15 residues of each docked complex, ranging from 0.32 to 1.87 nm across all instances. The assumption is made that the binding cavity remains robust and intact due to the reduced turbulence observed at the binding and active sites. The Rg values obtained from the gmxf_gyrate tool are utilized in the assessment of solidity and structural alterations in docked complexes. Additionally, it establishes the atomic mass that corresponds to the mass centers of the complex. The plumbagin-Caspase-3 complex exhibits average Rg values

ranging from 2.44 to 2.56 nm, and these values remain stable without any observable fluctuations for a duration of 50000 ps. Moreover, the correlation between Rg values and RMSD values of backbone C atoms provides evidence for the reliability of the selected protein-ligand complexes.

CONCLUSION

The focus of our investigation was the evaluation of plumbagin's potential as a caspase-3 activation within the context of Non-Small Cell Lung Cancer (NSCLC). Our research involved the utilization of molecular docking analyses and dynamic molecular simulations. These investigations have not only highlighted the remarkable anti-cancer properties of plumbagin in Non-Small Cell Lung Cancer (NSCLC), but have also suggested its potential to improve survival rates and decrease mortality by suppressing disease progression and prevalence. The efficacy of plumbagin as an anti-cancer agent against non-small cell lung cancer was confirmed through molecular docking analysis and molecular dynamics simulation studies. Hence, it has the potential to enhance the overall survival rate and mitigate mortality by focusing on the suppression or regulation of disease progression and prevalence. In our study, we have comprehensively examined the intricate relationship between emerging molecular knowledge, demonstrated through our utilization of molecular dynamics simulations, and a nuanced comprehension of the Absorption, Distribution, Metabolism, Excretion, and Toxicity (ADMET) properties of plumbagin. The convergence discussed not only establishes plumbagin as a strong contender deserving of additional investigation in the continuous quest for innovative therapeutic interventions, not limited to NSCLC but potentially applicable to various cancer types. Moreover, it highlights the ongoing progress in the development of groundbreaking cancer treatments. The aforementioned expedition exemplifies the potential of substances such as plumbagin, effectively bridging the gap between scientific findings in controlled environments and their practical implementation in medical settings. This development instills a sense of optimism in the ongoing and challenging endeavor to combat cancer.

DATA AVAILABILITY STATEMENT

The authors confirm that the data supporting the findings of this study are available within the article, including the supplementary file. Raw data that support the findings of this study are available from the corresponding authors upon request.

ACKNOWLEDGEMENT

This research has been funded by Scientific Research Deanship at the University of Hail, Saudi Arabia, through project number "RG-21052".

CONFLICT OF INTEREST

The authors declare that there is no conflict of interest.

SUMMARY

The activation potential of plumbagin is investigated against potential drug target of Non-Small Cell-Lung Carcinoma (NSCLC), Caspase-3. Systematic *in-silico* computational platforms are utilized for physico-chemical and ADMET properties characterization. Further, structural based molecular docking and MD simulation studies renders evidence of antagonist potential of plumbagin for Non-Small Cell-Lung Carcinoma (NSCLC) treatment.

REFERENCES

- Phan TN, Kim O, Ha MT, Hwangbo C, Min B-S, Lee J-H. Albnol B from mulberries exerts anti-cancer effect through mitochondria ROS production in lung cancer cells and suppresses *in vivo* tumor growth. *International journal of molecular sciences*. 2020;21(24):9502.
- Mahmoud AM, Al-Abd AM, Lightfoot DA, El-Shemy HA. Anti-cancer characteristics of mevinolin against three different solid tumor cell lines was not solely p53-dependent. *Journal of enzyme inhibition and medicinal chemistry*. 2012;27(5):673-9.
- Pandey P, Khan F, Chauhan P, Upadhyay TK, Bardakci F, Alam MJ, et al. Elucidation of the inhibitory potential of flavonoids against PKP1 protein in non-small cell lung cancer. *Cellular and Molecular Biology*. 2022;68(11):90-6.
- Smith HL, Southgate H, Tweddle DA, Curtin NJ. DNA damage checkpoint kinases in cancer. *Expert Reviews in Molecular Medicine*. 2020;22:e2.
- Siegel R, Ma J, Zou Z, Jemal A. *Cancer statistics, 2014*. CA: a cancer journal for clinicians. 2014;64(1):9-29.
- ACS ACS. *Cancer Facts & Figures*. Atlanta: American Cancer Society; 2020.
- Pandey P, Khan F, Upadhyay TK. Deciphering the modulatory role of apigenin targeting oncogenic pathways in human cancers. *Chemical Biology & Drug Design*. 2023.
- Sahoo G, Samal D, Khandayataray P, Murthy MK. A Review on Caspases: Key Regulators of Biological Activities and Apoptosis. *Molecular Neurobiology*. 2023:1-33.
- Lakshmi PJ, Kumar BS, Nayana RS, Mohan MS, Bolligarla R, Das SK, et al. Design, synthesis, and discovery of novel non-peptide inhibitor of Caspase-3 using ligand based and structure based virtual screening approach. *Bioorganic & medicinal chemistry*. 2009;17(16):6040-7.
- Asadi M, Taghizadeh S, Kaviani E, Vakili O, Taheri-Anganeh M, Tahamtan M, et al. Caspase-3: Structure, function, and biotechnological aspects. *Biotechnol Appl Biochem*. 2022;69(4):1633-45.
- Sharma S, Basu A, Agrawal R. Pharmacophore modeling and docking studies on some nonpeptide-based caspase-3 inhibitors. *BioMed Research International*. 2013;2013.
- D'Amelio M, Sheng M, Ceconi F. Caspase-3 in the central nervous system: beyond apoptosis. *Trends in neurosciences*. 2012;35(11):700-9.
- Hsu Y-L, Cho C-Y, Kuo P-L, Huang Y-T, Lin C-C. Plumbagin (5-hydroxy-2-methyl-1, 4-naphthoquinone) induces apoptosis and cell cycle arrest in A549 cells through p53 accumulation via c-Jun NH2-terminal kinase-mediated phosphorylation at serine 15 *in vitro* and *in vivo*. *Journal of Pharmacology and Experimental Therapeutics*. 2006;318(2):484-94.
- Panda M, Tripathi SK, Biswal BK. Plumbagin promotes mitochondrial mediated apoptosis in gefitinib sensitive and resistant A549 lung cancer cell line through enhancing reactive oxygen species generation. *Molecular Biology Reports*. 2020;47:4155-68.
- Wang CC, Chiang Y-M, Sung S-C, Hsu Y-L, Chang J-K, Kuo P-L. Plumbagin induces cell cycle arrest and apoptosis through reactive oxygen species/c-Jun N-terminal kinase pathways in human melanoma A375. S2 cells. *Cancer letters*. 2008;259(1):82-98.
- Tripathi SK, Rengasamy KR, Biswal BK. Plumbagin engenders apoptosis in lung cancer cells via caspase-9 activation and targeting mitochondrial-mediated ROS induction. *Archives of pharmaceutical research*. 2020;43:242-56.
- Liu H, Zhang W, Jin L, Liu S, Liang L, Wei Y. Plumbagin Exhibits Genotoxicity and Induces G2/M Cell Cycle Arrest via ROS-Mediated Oxidative Stress and Activation of ATM-p53 Signaling Pathway in Hepatocellular Cells. *International journal of molecular sciences*. 2023;24(7):6279.
- Alshahrani MY, Alshahrani KM, Tasleem M, Akeel A, Almeleebia TM, Ahmad I, et al. Computational Screening of Natural Compounds for Identification of Potential Anti-Cancer Agents Targeting MCM7 Protein. *Molecules*. 2021;26(19):5878.
- Jumper J, Evans R, Pritzel A, Green T, Figurnov M, Ronneberger O, et al. Highly accurate protein structure prediction with AlphaFold. *Nature*. 2021;596(7873):583-9.
- PubChem Compound Summary for CID 10205, Plumbagin [Internet]. PubChem [Internet]. Bethesda (MD). [cited January 6, 2021]. Available from: <https://pubchem.ncbi.nlm.nih.gov/compound/Plumbagin>.

21. Wang Y, Xiao J, Suzek TO, Zhang J, Wang J, Bryant SH. PubChem: a public information system for analyzing bioactivities of small molecules. *Nucleic acids research*. 2009;37(suppl_2):W623-W33.
22. Tasleem M, Alrehaily A, Almeleebia TM, Alshahrani MY, Ahmad I, Asiri M, et al. Investigation of Antidepressant Properties of Yohimbine by Employing Structure-Based Computational Assessments. *Curr Issues Mol Biol*. 2021;43(3):1805-27.
23. Daina A, Michielin O, Zoete V. SwissADME: a free web tool to evaluate pharmacokinetics, drug-likeness and medicinal chemistry friendliness of small molecules. *Sci Rep*. 2017;7(1):42717.
24. Morris GM, Huey R, Lindstrom W, Sanner MF, Belew RK, Goodsell DS, et al. AutoDock4 and AutoDockTools4: Automated docking with selective receptor flexibility. *Journal of computational chemistry*. 2009;30(16):2785-91.
25. Rigsby RE, Parker AB. Using the PyMOL application to reinforce visual understanding of protein structure. *Biochemistry and Molecular Biology Education*. 2016;44(5):433-7.
26. Kumari A, Shrivastava N, Mishra M, Somvanshi P, Grover A. Inhibitory mechanism of an antifungal drug, caspofungin against amyloid β peptide aggregation: Repurposing via neuroinformatics and an experimental approach. *Molecular and Cellular Neuroscience*. 2021;112:103612.
27. Van Der Spoel D, Lindahl E, Hess B, Groenhof G, Mark AE, Berendsen HJ. GROMACS: fast, flexible, and free. *Journal of computational chemistry*. 2005;26(16):1701-18.
28. Rajendran BK, Suresh MX, Bhaskaran S, Harshitha Y, Gaur U, Kwok H. Pharmacoinformatic Approach to Explore the Antidote Potential of Phytochemicals on Bungarotoxin from Indian Krait, *Bungarus caeruleus*. *Computational and Structural Biotechnology Journal*. 2018;16:450-61.
29. Tasleem M, Alrehaily A, Almeleebia TM, Alshahrani MY, Ahmad I, Asiri M, et al. Investigation of Antidepressant Properties of Yohimbine by Employing Structure-Based Computational Assessments. *Current Issues in Molecular Biology*. 2021;43(3):1805-27.
30. Lobell M, Sivarajah V. *In silico* prediction of aqueous solubility, human plasma protein binding and volume of distribution of compounds from calculated pKa and AlogP98 values. *Molecular diversity*. 2003;7:69-87.
31. (2023). NCFBI. PubChem Compound Summary for CID 5702546, Resiniferatoxin [Available from: <https://pubchem.ncbi.nlm.nih.gov/compound/5702546>].
32. Burley SK, Bhikadiya C, Bi C, Bittrich S, Chen L, Crichlow GV, et al. RCSB Protein Data Bank: powerful new tools for exploring 3D structures of biological macromolecules for basic and applied research and education in fundamental biology, biomedicine, biotechnology, bioengineering and energy sciences. *Nucleic Acids Research*. 2020;49(D1):D437-51.
33. Pu Q, Han Z, Li X, Li Q, Li Y. Designing and screening of fluoroquinolone substitutes using combined *in silico* approaches: biological metabolism-bioconcentration bilateral selection and their mechanism analyses. *Green Chemistry*. 2022;24(9):3778-93.
34. Jena L, Nayak U. Theories of Career Development: An analysis. 2020.
35. Fatima S, Gupta P, Sharma S, Sharma A, Agarwal SM. ADMET profiling of geographically diverse phytochemical using chemoinformatic tools. *Future Med Chem*. 2020;12(1):69-87.
36. Chandra A, Chaudhary M, Qamar I, Singh N, Nain V. *In silico* identification and validation of natural antiviral compounds as potential inhibitors of SARS-CoV-2 methyltransferase. *J Biomol Struct Dyn*. 2021:1-11.
37. Meng XY, Zhang HX, Mezei M, Cui M. Molecular docking: a powerful approach for structure-based drug discovery. *Curr Comput Aided Drug Des*. 2011;7(2):146-57.
38. Majewski M, Ruiz-Carmona S, Barril X. An investigation of structural stability in protein-ligand complexes reveals the balance between order and disorder. *Communications Chemistry*. 2019;2(1):110.
39. Bradley SH, Kennedy MP, Neal RD. Recognising lung cancer in primary care. *Advances in therapy*. 2019;36:19-30.
40. Lim RB. End-of-life care in patients with advanced lung cancer. *Therapeutic advances in respiratory disease*. 2016;10(5):455-67.
41. Lemjabbar-Alaoui H, Hassan OU, Yang Y-W, Buchanan P. Lung cancer: Biology and treatment options. *Biochimica et Biophysica Acta (BBA)-Reviews on Cancer*. 2015;1856(2):189-210.
42. Fan H, Shao Z-Y, Xiao Y-Y, Xie Z-H, Chen W, Xie H, et al. Incidence and survival of non-small cell lung cancer in Shanghai: a population-based cohort study. *BMJ open*. 2015;5(12):e009419.
43. Cicali EJ, Smith DM, Duong BQ, Kovar LG, Cavallari LH, Johnson JA. A Scoping Review of the Evidence Behind Cytochrome P450 2D6 Isoenzyme Inhibitor Classifications. *Clin Pharmacol Ther*. 2020;108(1):116-25.
44. Trainor GL. The importance of plasma protein binding in drug discovery. *Expert opinion on drug discovery*. 2007;2(1):51-64.
45. Saeed M, Tasleem M, Shoaib A, Alabdallah NM, Alam MJ, El Asmar Z, et al. Investigation of antidiabetic properties of shikonin by targeting aldose reductase enzyme: *In silico* and *in vitro* studies. *Biomed Pharmacother*. 2022;150:112985.
46. Rizeq B, Gupta I, Ilesanmi J, AlSafran M, Rahman MM, Ouhtit A. The power of phytochemicals combination in cancer chemoprevention. *Journal of Cancer*. 2020;11(15):4521.
47. Zhao Y, Lin X, Zeng W, Qin X, Miao B, Gao S, et al. Berberine inhibits the progression of renal cell carcinoma cells by regulating reactive oxygen species generation and inducing DNA damage. *Molecular Biology Reports*. 2023:1-11.
48. Rahman MM, Islam MR, Akash S, Shohag S, Ahmed L, Supti FA, et al. Naphthoquinones and derivatives as potential anticancer agents: An updated review. *Chemico-Biological Interactions*. 2022;368:110198.
49. Yin Z, Zhang J, Chen L, Guo Q, Yang B, Zhang W, et al. Anticancer effects and mechanisms of action of plumbagin: review of research advances. *BioMed Research International*. 2020;2020.
50. Seshadri P, Rajaram A, Rajaram R. Plumbagin and juglone induce caspase-3-dependent apoptosis involving the mitochondria through ROS generation in human peripheral blood lymphocytes. *Free Radical Biology and Medicine*. 2011;51(11):2090-107.
51. Aziz MH, Dreckschmidt NE, Verma AK. Plumbagin, a medicinal plant-derived naphthoquinone, is a novel inhibitor of the growth and invasion of hormone-refractory prostate cancer. *Cancer research*. 2008;68(21):9024-32.
52. Kuo P-L, Hsu Y-L, Cho C-Y. Plumbagin induces G2-M arrest and autophagy by inhibiting the AKT/mammalian target of rapamycin pathway in breast cancer cells. *Molecular cancer therapeutics*. 2006;5(12):3209-21.
53. Ahmad A, Banerjee S, Wang Z, Kong D, Sarkar FH. Plumbagin-induced apoptosis of human breast cancer cells is mediated by inactivation of NF- κ B and Bcl-2. *Journal of cellular biochemistry*. 2008;105(6):1461-71.
54. Sandur SK, Ichikawa H, Sethi G, Ahn KS, Aggarwal BB. Plumbagin (5-hydroxy-2-methyl-1, 4-naphthoquinone) suppresses NF- κ B activation and NF- κ B-regulated gene products through modulation of p65 and I κ B α kinase activation, leading to potentiation of apoptosis induced by cytokine and chemotherapeutic agents. *Journal of Biological Chemistry*. 2006;281(25):17023-33.
55. Jamal MS, Parveen S, Beg MA, Suhail M, Chaudhary AG, Damanhour GA, et al. Anticancer compound plumbagin and its molecular targets: a structural insight into the inhibitory mechanisms using computational approaches. *PloS one*. 2014;9(2):e87309.
56. Liang Y, Zhou R, Liang X, Kong X, Yang B. Pharmacological targets and molecular mechanisms of plumbagin to treat colorectal cancer: a systematic pharmacology study. *European Journal of Pharmacology*. 2020;881:173227.
57. Mander S, Gorman GS, Coward LU, Christov K, Green A, Das Gupta TK, et al. The brain-penetrant cell-cycle inhibitor p28 sensitizes brain metastases to DNA-damaging agents. *Neuro-Oncology Advances*. 2023;5(1):vdad042.
58. Ye L-y, Sun L-x, Zhong X-h, Chen X-s, Hu S, Xu R-r, et al. The structure of blood-tumor barrier and distribution of chemotherapeutic drugs in non-small cell lung cancer brain metastases. *Cancer Cell International*. 2021;21:1-12.
59. Angeli E, Nguyen TT, Janin A, Bousquet G. How to make anticancer drugs cross the blood-brain barrier to treat brain metastases. *International journal of molecular sciences*. 2019;21(1):22.
60. Inno A, Di Noia V, D'Argento E, Modena A, Gori S. State of the art of chemotherapy for the treatment of central nervous system metastases from non-small cell lung cancer. *Translational lung cancer research*. 2016;5(6):599.
61. TA V. Molecular Docking: From Lock and Key to Combination Lock. *J Mol Med Clin Appl*. 2018;2(1):10-16966.

Cite this article: Saeed M, Tasleem M, Upadhyay TK, Bhardwaj T, Siddiqui S, Alam MJ, et al. Exploring the Potential of Plumbagin as an Activator of Caspase 3 for Non-small Cell Lung Carcinoma: A Comprehensive *in silico* Study. *Indian J of Pharmaceutical Education and Research*. 2024;58(2):526-34.